Color Appearance and the Digital Imaging Pipeline

Brian A. Wandell
Psychology Department
Stanford University, Stanford, CA 94305
wandell@stanford.edu
http://pdc.stanford.edu

Abstract

An effective image reproduction pipeline, spanning image capture, processing and display, must be designed to account for the properties of the human observer. In designing an image pipeline, three principles of human vision are particularly important: trichromacy, color adaptation, and pattern-color sensitivity. These properties also play an important role in metrics used to evaluate image quality reproduction.

The main portion of this review comprises a description of these properties of the visual system and how these principles are incorporated into the image reproduction pipeline. The last part of this review describes a new image capture technology, based on a digital pixel fabricated on a CMOS process. This sensor is well-designed for exploring a novel image pipeline architecture that we call multiple-capture, single-image. This architecture is being developed to serve features of human vision that are not yet incorporated in the conventional pipeline.

1. Introduction

The last several years have been a time of rapid growth in the design and implementation of devices used for color reproduction. To reproduce color images requires that these devices work as part of a general imaging pipeline, and that the algorithms implemented within these devices manage the image information so that the appearance of the original and the final reproduction are similar to a human observer.

The need to design the imaging pipeline with respect to properties of the visual pathways is widely appreciated in the engineering community. However, the connection between the basic properties of human vision and the design of digital imaging devices can be hard to discern. In large part this is because when considering the many engineering design systems and the many properties of human vision, drawing the relationship between the two can be daunting.

In the main portion of this review, I describe three fundamental properties of the human visual system that are directly relevant to the image system pipeline: trichromacy, light adaptation, and pattern-color sensitivity. I describe the empirical basis of these properties, and how these fundamental empirical observations are used in the design imaging systems.

In the final paragraphs, I introduce our explorations of architectural principles of human visual encoding that may be a useful guide the development of digital imaging architectures. The principle is based on the observation that the cone mosaic absorptions are converted to signals carried by a multiplicity of neural mosaics; each mosaic represents the entire visual field. The neurons in these mosaics have receptive fields that are specialized to measure different aspects of the image. Some mosaics are better suited to represent motion and others pattern; some mosaics carry control signals for accommodation and others to direct eye position. We are exploring an engineering architecture, *multiple-capture, single-image* (MCSI), that creates multiple image representations but ultimately produces a single output image. I will describe one implementation of a CMOS imager and preliminary work with the MCSI architecture.

2. Color Fundamentals

2.1 The Cone Mosaic

Human vision begins by the absorption of photons by the photopigments contained in the rod and cone retinal receptors. Color vision depends on signals within the three types of cone receptors that comprise three spatial mosaics. Recently, it has become possible to image the cone mosaics in the living human eye using methods from adaptive optics [1]. It is instructive to compare the size, density and distribution of the cones with that of image sensors in current digital imaging devices.

The cones are present at their highest spatial density in central vision (central fovea, less than 0.5 deg from

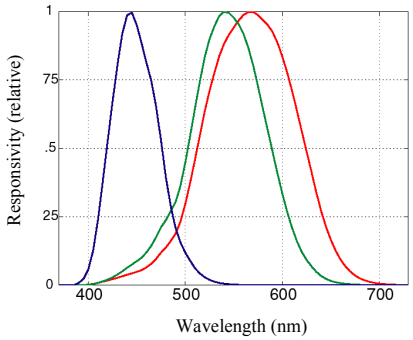

Figure 1. The wavelength absorption functions of the long (L), middle (M), and short (S) human cone photopigments as derived by [2]. These curves include the effects of the optics and ocular pigments. Color matches within a single context can be determined using these three curves.

fixation). The size and sampling density of the cone photoreceptors varies considerably from the fovea to the periphery.

In the central fovea, the cones sample the image at a rate of roughly 120 cones per linear degree of visual angle in the central fovea. Hence, the central portion of the visual field is sampled by approximately 10^4 cones per square degree. The sampling rate reduces dramatically with distance from the fovea, so that the full visual field, spanning roughly 160 x 135 deg, is sampled by only 5 x 10^5 cones in each eye, producing an average sampling rate that is much lower: $2x10^2$ per square degree.

By comparison, modern digital cameras typically capture an image a scene spanning 35x35 deg of visual angle. These cameras often have roughly $2x10^6$ pixels and thus sample the image at $1.5x10^3$ pixels per square degree. This sampling rate exceeds the average sampling density of the cone mosaic in the human eye, though the foveal human sampling density in the is roughly an order of magnitude higher. To achieve the foveal sampling density throughout the camera field of view would require a sensor with $1.2x10^7$ pixels.

Twelve million pixels per image is more than can be supported by other devices in the imaging pipeline (displays and printers). While there may be some applications that require this density, it is not yet of practical significance for current consumer imaging.

2.2 The Photopigment Absorption Curves

Differences in the wavelength responsivity of the three types of cone photopigments provide the key mechanism that enables discrimination of light based on wavelength composition. The spectral absorption functions of the cone photopigments set a fundamental limit on how much information is available to make this discrimination. Consider how the human visual system might discriminate the wavelength composition between two uniform patches of light. With such stimuli, the discrimination must be made by comparing the average cone photopigment absorption rates caused by the patches.

To perform this computation, we begin with the relative wavelength responsivity of the three cone photopigment functions (including media losses). These functions, derived from an analysis of behavioral data, are shown in Figure 1 [2]. The absorption functions are denoted as $L(\lambda)$, $M(\lambda)$, and $S(\lambda)$, where the letters are chosen to describe the relative position of the peak sensitivity: long, middle and short-wavelength. For computational purposes, it is useful to represent these functions at sampled values spanning the visual range, say from 370 to 770 nm sampled every 5 nm. Using this format, the rate of photopigment absorptions caused by a test light, represented by the column vector E, can be computed as the inner product of E and the photopigment absorption function. To perform this computation, it is convenient to group the three photopigment absorption functions into the columns of a matrix, **P**. The absorption in the three cone types caused by a test light is the matrix product $\mathbf{P}^t\mathrm{E}$. Two different test lights, E and E', cause the same photopigment absorption rates when $\mathbf{P}^t\mathrm{E} = \mathbf{P}^t\mathrm{E}'$, or equivalently when their difference, (E – E'), is in the null space of $\mathbf{P}^t$.

Knowledge of the absorption properties of the photopigments, represented in the matrix **P,** has been a very important aspect of image system design. The columns of this matrix are called the *color-matching functions.* Notice that to predict whether two lights cause the same rate of photopigment absorptions in the three types of cone photopigments, it is only essential to know the color-matching functions up to a linear transformation: If **M** is a 3x3 non-singular matrix, then $\mathbf{MP}^t\mathrm{E} = \mathbf{MP}^t\mathrm{E}'$ if and only if $\mathbf{P}^t\mathrm{E} = \mathbf{P}^t\mathrm{E}'$.

A set of color-matching functions was standardized in the 1931 meeting of the CIE [3], and this standard is still in use today [4, 5]. Coupling the behaviorally determined color-matching functions to the responses of individual cones [6, 7], followed by the discovery of the genetic code for the pigments is a spectacular achievement of visual neuroscience [8].

2.3 Color Metrics

Perhaps the most important application of the color-matching functions is their use in selecting the outputs of

display media to reproduce the color of an original. Display media, including CRTs, LCDs, and prints, do not reproduce the spectral signal of an original; rather, given an original signal, E, image processing methods are used to select a display signal, say E', that is visually similar to the original. There are a number of factors that must be considered in selecting this signal. But, in the special case when the viewing conditions of the original and the reproduction are the same, the key condition is that $\mathbf{P}^t$E should be "close" to $\mathbf{P}^t$E'.

For the engineer, the usual definition of "close" is to measure the mean squared error. However, this is a very poor measure of color differences. The poor quality of a squared error measure is illustrated by the iso-discrimination contour shown in Figure 2. The contour shows perturbations of the (L,M) cone coordinates that are equally detectable from the background (plotted at the origin of the graph). The detection contour is very far from a circle. Rather, the observer is far more sensitive to some color directions than others.

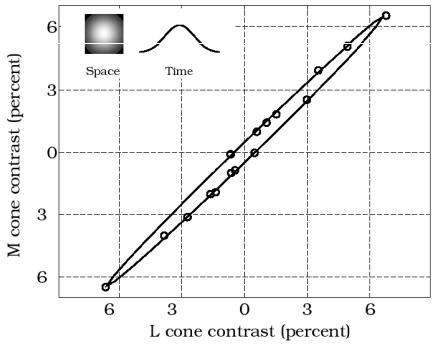

Figure 2. A detection contour within the L,M plane. The target was a low spatial and temporal frequency probe presented on a steady background. The cone coordinates describe the deviation of the probe from the background. The highly elliptical shape shows that mean-squared-error is a poor description of the perception of color differences. After [4, Figure 9.15]

Rather than using squared error in cone coordinates, the CIE recommends a metric formula (CIELAB) that is based on squared-error following a nonlinear transformation of the cone coordinates [9, 10]. The CIELAB metric difference between a pair of points is computed using three input quantities: the two vectors, $\mathbf{P}^t$E and $\mathbf{P}^t$E', and another vector that represents the ambient illumination conditions (the white point). The CIELAB color difference metric is in wide use for specifying color precision in contracts and in evaluating the reproduction capabilities of imaging systems.

3. Color Adaptation

3.1 Adaptation Phenomena

The color-matching functions and the CIELAB metric have been enormously valuable tools in designing imaging systems. These tools offer excellent guidance for creating appearance between objects seen in the same viewing context. When objects are compared in different viewing contexts, however, the color-matching functions alone are not enough.

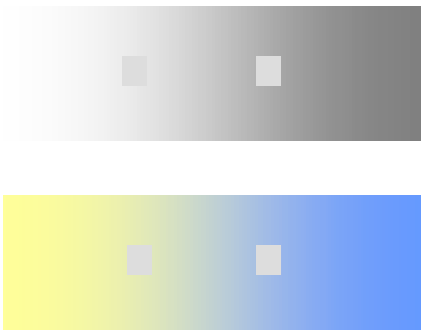

Figure 3. The appearance of a target depends on its viewing context. The four squares shown in this figure are physically identical. Differences in their appearance occur because they are presented in different contexts. (The illusion on the bottom is in color.) After [4, Figure 9.1]

Simple visual illusions provide good examples to illustrate the limits of these calculations. Figure 3 shows four small squares that are physically the same; yet because they are seen in different contexts the appearance of the squares differs. This well-known illusion demonstrates that color reproduction using only the point by point photopigment absorptions need not produce satisfactory appearance matches. In general, image reproduction must take into account the entire spatial distribution of cone absorptions, not just the values at corresponding points.

Efforts to understand the general principles of image interpretation and specifically brightness judgments have produced many wonderful illusions and interesting theoretical ideas [11-13]. But, these have not yet become practical engineering tool applicable to the imaging pipeline.

There has been progress, however, in understanding the consequence of simple context changes, as in Figure 3.

Understanding these context changes are of practical significance because they mirror certain natural context differences: Suppose a target is measured in a blue skylight (right half of the lower image). A target reproduced directly under an illuminant like the disk of the sun (left half of lower image) will not match if the reproduction slavishly equates their photopigment absorptions. Rather, the reproduction must take into account the new context as well as the color-matching functions. The correction procedure for simple changes in the mean image level, usually caused by differences in ambient lighting, is part of the many digital imaging pipelines and is called color balancing.

3.2 Adaptation Experiments

The experimental basis for choosing how to color balance is the asymmetric color-matching experiment is

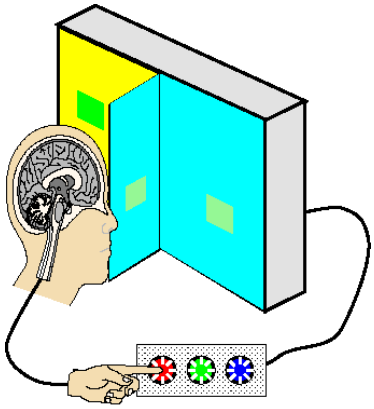

Figure 4. In the asymmetric color-matching experiment an observer adjusts a target presented in a standard context (match) so that its appearance is the same as a target shown in a different context (test). The experiment illustrated here shows a binocular form of the experiment. After a figure in [14].

illustrated in Figure 4. Subjects adjust the appearance of a target presented in a standard condition in order to match the appearance of various targets shown in a different context. By measuring a collection of such matches, one can find a function that converts cone absorptions in one context into cone absorptions with the same appearance presented in a standard condition. Then, by additional experiments, one can estimate how the function covaries with the viewing context.

3.3 Computing the Effect of Adaptation

Asymmetric color-matching experiments to date have tested only a modest range of conditions; there is much more to learn about such matches. As a first approximation, however, the matching between conditions appears to follow the simple rule. First, in the simple experimental arrangement using a uniform field and a test that is a modulation of that field (Figure 4), we can express the test and matching probes as deviations from the steady background: $t = (\Delta L', \Delta M', \Delta S')$ and $m = (\Delta L, \Delta M, \Delta S)$. These quantities are expressed in cone coordinates. A simple coordinate scaling, $(\rho(c)\ \Delta L, \gamma(c)\ \Delta M, \beta(c)\ \Delta S)$, approximates the match, where $\rho(c)$, $\gamma(c)$ and $\beta(c)$ are real scale factors that depend on the context, c. This simple scalar relationship has been verified in a large set of asymmetric matching experiments that measure the effect of changes in the mean field (e.g. [14-20]).

An important and unsolved problem concerning how one might generalize these experimental matches is this: we do not know how to compute the scale factors, $\rho(c)$, $\gamma(c)$ and $\beta(c)$, from knowledge of the image. While it is possible to verify for any particular image that the functional relationship approximately holds, we do not know how to begin with a complex image and predict the scale factors. For this reason, engineering applications make simple approximations (e.g., the scale factors are inversely proportional to the mean absorption levels). These rules are not correct and lead to some noticeable errors in reproductions.

There are two cautionary notes to be sounded. First, the range of viewing conditions that has been tested is very modest compared to the range of natural images. Even within this range, several failures have been demonstrated [17-19, 21]. To date, these failures are described as deviations from the simple scaling. It is possible that new stimulus configurations will be found that will reveal substantial failures in general with this rule serving only as a special case for uniform backgrounds.

Second, it is important to recognize that the scaling rule applies to a unique coordinate frame: the cone coordinates. It is not equivalent to scale in a different coordinate frame (e.g., CIELAB coordinates, or linear transformations of the cone coordinates). When direct comparison with experimental measurements have been made, scaling in other coordinate frames does not predict the data as well.

4. Pattern and Color

4.1 Pattern-Color Phenomena

Temporal and spatial structure of a stimulus also strongly influences color appearance. While people are trichromatic when viewing low spatial and temporal frequency targets (below 20 cycles per degree and 20 Hz), above this range we become monochromats. The phenomenon is well-known to television engineers who

relied upon this observation when adapting transmission standards: the chromatic signals are sent at very low spatial bandwidth. Poor color resolution is also an important element of compression standards, such as that used in JPEG. The color channels are compressed much more aggressively than the luminance channels. The phenomena can be found illustrated in several places (e.g., [4, Color Plate 7]).

Several labs have measured human pattern and color sensitivity [22-25], but only a few measurements of asymmetric color matches comparing targets with different spatial or temporal structure [26-29]. At present, two summary statements appear to hold.

First, the asymmetric pattern matches are not explained by a scaling of cone signals. Instead, these matches are better predicted by first transforming the cone representation into a new coordinate frame, and then scaling the results. The spectral curves defining the new coordinate frame derived from experimental measurements [23, 26, 27] are shown in Figure 5. These curves are similar to opponent-color curves derived from very different color appearance experiments [27, 30, 31].

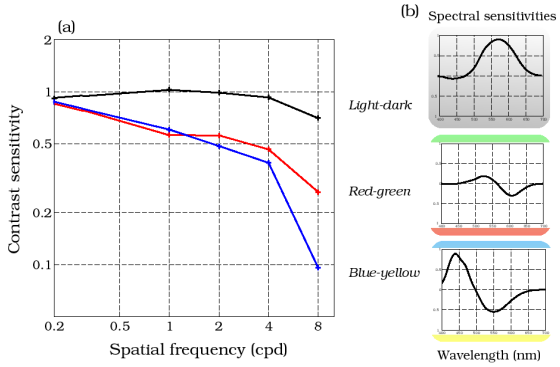

Figure 5. Pattern asymmetric color matches can be predicted by a pattern-color separable model. The color coordinate frame, however, is a linear transformation away from the cone coordinates. The curves defining (a) the spatial modulation transfer functions and (b) corresponding color mechanisms are shown. Both sets of curves were derived from the measurements.

Second, the pattern-color results can be modeled using a pattern-color separable model. Specifically, one can separate the color and pattern transformations into different stages of the model. This makes it practical to build metrics that analyze the reproduction accuracy of full image data.

4.3 Application: Pattern-Color Metrics

Zhang and I developed and tested a pattern-color metric, Spatial-CIELAB (S-CIELAB) using the empirical measurements of pattern-color appearance and sensitivity [32-35]. An overview of the metric calculation is shown in Figure 6. This metric was designed to be compatible with the CIELAB metric when applied to uniform targets. It also was designed to be pattern-color separable in order to make the metric practical for application to complex images.

A Matlab implementation of the metric can be obtained from the Internet http://white.stanford.edu . An on-line application of this metric is used at http://vischeck.com.

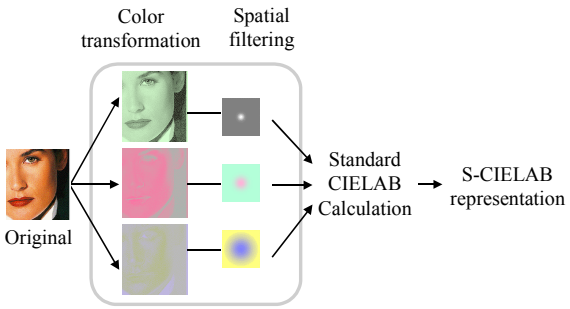

Figure 6. The Spatial-CIELAB metric (S-CIELAB) includes pattern and color sensitivity in a single metric. The metric is designed to be pattern-color separable [26] and compatible with the standard CIELAB calculation applied to uniform fields [36].

5. Designing Digital Imaging Architectures

The elements of human vision I have described mainly illustrate visual limitations: trichromacy allows imaging systems to ignore most of the spectral signal; pattern and temporal sensitivity limits reduce the need to allocate bandwidth in the imaging pipeline. Yet, the visual system achieves some remarkable success in achieving various types of visual tasks. In this final section, I will consider an image pipeline design principle that attempts to copy one of the strengths of human vision.

The retinal cones each send their output to multiple types of neurons. Collections of these neurons, in turn, form a set of spatial mosaics that tile the image plane. The neurons within the separate mosaics are interleaved within the retina, but they can be distinguished by a variety of properties, including cell morphology, receptive

field properties, and axonal destinations in the central visual pathways. Based on these differences it appears that these mosaics are specialized for different computations (e.g., motion, pattern, color) and control functions (e.g., pupil, eye movement) . These mosaics appear to represent multiple captures of the cone mosaics; the neural mosaics each perform different analytical functions. Their joint output results in a single, perceived image.

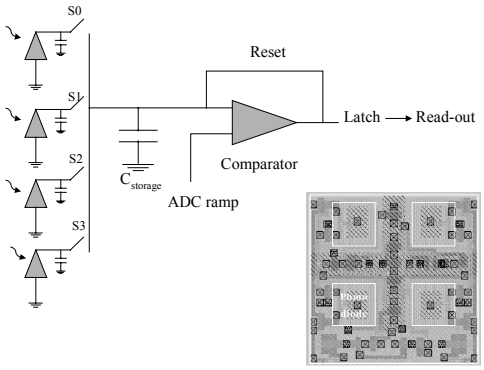

Figure 7. An implementation of a digital pixel sensor (DPS) is shown in schematic form (a) and in layout form (b). Four photodiodes share a single programmable ADC. The pixel outputs can be spatially pooled prior to read-out and multiple temporal samples can be obtained while the pixels are charging in response to light [37, 38].

As is often the case when comparing digital hardware with neural tissue, it is possible to trade processing speed for spatial parallelism. The digital pixel sensor designed by El Gamal's group [37, 38] is well-suited to exploring an architecture based on multiple representations (see Figure 7). In this architecture, each pixel has a separate analog-to-digital converter (ADC). As a group, the sensor ADCs can be programmed between frames, making it possible to acquire a series of images with different spatial and temporal properties. Because the pixel data are digital, they can be transferred into memory very quickly; because the sensor is fabricated using a 0.35 micron CMOS process, the memory and other architectural elements needed to integrate data from multiple frames can reside on the sensor itself. Hence, the sensor provides an opportunity to experiment with the multiple capture, single image architecture.

One application where the MCSI architecture is helpful is in extending the system's dynamic range. In the CMOS sensor, the ADC samples the charging photodiode without destroying the charge. Hence, it is possible to measure the signal at several moments in time without resetting the sensor. With the fast readout, it is possible to store these multiple samples, creating an architecture that captures the image at several different exposure durations. This architecture increases the system's dynamic range beyond what can be obtained from a single measurement of the photodiode itself. Other applications have been implemented, and many more should be possible [38].

6. Conclusions

Image systems pipelines have benefited from an understanding of the basic properties of the visual pathways; further measurements of visual sensitivity will continue to lead to improvements in the quality of digital imaging devices.

The creation of imaging devices with novel properties also offers opportunities to develop new areas of vision research. The next generations of imagers, such as those based on digital pixels, provide an opportunity for developing our understanding in order to create increasingly precise and beautiful images. In addition to new sensors, many new methods for displaying images are being developed now, and these too offer challenges and opportunities for future research that combines technology and visual neuroscience. In imaging, the future is always bright.

7. References

[1] A. Roorda and D. R. Williams, "The arrangement of the three cone classes in the living human eye [see comments]," *Nature*, vol. 397, pp. 520-2, 1999.

[2] A. Stockman and L. T. Sharpe, "Cone spectral sensitivities and color matching.," in *Color Vision: from genes to perception*, K. S. Gegenfurtner, L.T., Ed. Cambridge: Cambridge University Press, 1999, pp. 53-88.

[3] "CIE Proceedings," presented at Commission Internationale D'Eclairage, Cambridge, England, 1931.

[4] B. A. Wandell, *Foundations of Vision*. Sunderland, MA: Sinauer Press, 1995.

[5] R. S. Berns, *Billmeyer and Saltzman's Principles of Color Technology (3rd Edition)*. New York: John Wiley and Sons, 2000.

[6] D. A. Baylor, B. J. Nunn, and J. L. Schnapf, "Spectral sensitivity of cones of the monkey Macaca fascicularis," *J. Physiol.*, vol. 390, pp. 145-160, 1987.

[7] J. L. Schnapf, T. W. Kraft, and D. A. Baylor, "Spectral sensitivity of human cone

photoreceptors," *Nature*, vol. 325, pp. 439-441, 1987.

[8] J. Nathans, T. P. Piantanida, R. L. Eddy, T. B. Shows, and D. S. Hogness, "Molecular genetics of inherited variation in human color vision," *Science*, vol. 232, pp. 203-210, 1986.

[9] I. C. o. I. (CIE), "Recommendations on uniform color spaces, color difference equations, psychometric color terms," , Vienna 1978.

[10] I. C. o. I. (CIE), "Industrial Colour-Difference Evaluation," , Vienna 1995.

[11] E. H. Adelson, "Perceptual organization and the judgment of brightness," *Science*, vol. 262, pp. 2042-2044, 1993.

[12] K. Nakayama and S. Shimojo, "Experiencing and perceiving visual surfaces," *Science*, vol. 257, pp. 1357-63, 1992.

[13] A. Gilchrist and V. Ramachandran, "Red Rooms in White Light Appear Different from White Rooms in Red Light," *Invest. Opthal.*, vol. 33, pp. 314A, 1992.

[14] E. J. Chichilnisky and B. A. Wandell, "Photoreceptor sensitivity changes explain color appearance shifts induced by large uniform backgrounds in dichoptic matching [see comments]," *Vision Res*, vol. 35, pp. 239-54, 1995.

[15] D. H. Brainard and B. A. Wandell, "Asymmetric color matching: how color appearance depends on the illuminant," *J. Opt. Soc. A.*, vol. 9, pp. 1433-1448, 1992.

[16] D. H. Brainard, W. A. Brunt, and J. M. Speigle, "Color constancy in the nearly natural image. I. Asymmetric matches," *J Opt Soc Am A*, vol. 14, pp. 2091-110, 1997.

[17] E. J. Chichilnisky and B. A. Wandell, "Seeing gray through the ON and OFF pathways," *Visual Neurosci*, vol. 13, pp. 591-6, 1996.

[18] K. H. Bauml, "Simultaneous color constancy: how surface color perception varies with the illuminant," *Vision Res*, vol. 39, pp. 1531-50, 1999.

[19] P. B. Delahunt and D. H. Brainard, "Control of chromatic adaptation: Signals from separate cone classes interact," *Vision Research*, (in press).

[20] J. S. Werner and J. Walraven, "Effect of chromatic adaptation on the achromatic locus: the role of contrast, luminance and background color," *Vision Res*, vol. 22, pp. 929-43, 1982.

[21] R. Mausfeld and R. Niederee, "An inquiry into relational concepts of colour, based on incremental principles of colour coding for minimal relational stimuli," *Perception*, vol. 22, pp. 427-462, 1993.

[22] E. M. Granger and J. C. Heurtley, "Visual chromatic modulation transfer function," *J. Opt. Soc. Am.*, vol. 63, pp. 73-74, 1973.

[23] A. B. Poirson and B. A. Wandell, "Pattern-color separable pathways predict sensitivity to simple colored patterns," *Vision Res*, vol. 36, pp. 515-26, 1996.

[24] K. Mullen, "The constrast sensitivity of human colour vision to red-green and blue-yellow chromatic gratings," *J. Physiol.*, vol. 359, pp. 381-400, 1985.

[25] N. Sekiguchi, D. R. Williams, and D. H. Brainard, "Aberration-free measurements of the visibility of isoluminant gratings," *J Opt Soc Am A*, vol. 10, pp. 2105-17, 1993.

[26] A. B. Poirson and B. A. Wandell, "The appearance of colored patterns: pattern-color separability," *J. Opt. Soc. Am. A*, vol. 10, pp. 2458-2471, 1993.

[27] K. H. Bauml and B. A. Wandell, "Color appearance of mixture gratings," *Vision Res*, vol. 36, pp. 2849-64, 1996.

[28] B. Singer and M. D'Zmura, "Contrast gain control: a bilinear model for chromatic selectivity," *J Opt Soc Am A*, vol. 12, pp. 667-85, 1995.

[29] B. Wandell, "Color Appearance: The Effects of Illumination and Spatial Resolution," *Proc. Nat. Acad. Sci.*, vol. 90, pp. 1494-1501, 1993.

[30] E. Hering, "Outlines of a Theory of the Light Sense," , 1964.

[31] E. J. Chichilnisky and B. A. Wandell, "Trichromatic opponent color classification," *Vision Res*, vol. 39, pp. 3444-58, 1999.

[32] X. Zhang and B. A. Wandell, "A spatial extension to CIELAB for digital color image reproduction," in *Society for Information Display Symposium Technical Digest*, vol. 27, 1996, pp. 731-734.

[33] X. Zhang, J. E. Farrell, and B. A. Wandell, "Applications of S-CIELAB: A spatial extension to CIELAB," in *Proceedings of the {IS\&T/SPIE} 9th Annual Symposium on Electronic Imaging*, 1997.

[34] X. Zhang, E. Setiawan, and B. A. Wandell, "Image distortion maps," in *Final Program and Proceedings of the Fifth {IS\&T/SID} Color Imaging Conference. Color Science, Systems and Applications*. Scottsdale, AZ, USA, 1997, pp. 120-125.

[35] X. Zhang, D. A. Silverstein, J. E. Farrell, and B. A. Wandell, "Color image quality metric S-CIELAB and its application on halftone texture visibility," in *{COMPCON97} Digest of Papers*, 1997, pp. 44-48.

[36] X. Zhang and B. A. Wandell, "A spatial extension to CIELAB for digital color image reproduction," *Society for Information Display Symposium Technical Digest*, vol. 27, pp. 731-734, 1996.

[37] D. X. D. Yang, A. El Gamal, B. Fowler, and H. Tian, "A 640*512 CMOS image sensor with ultra wide dynamic range floating-point pixel-level ADC," presented at 1999 IEEE International Solid-State Circuits Conference, San Francisco, CA, USA, 1999.

[38] B. Wandell, P. Catrysse, J. DiCarlo, D. Yang, and A. E. Gamal, "Multiple Capture Single Image with a CMOS Sensor," presented at Chiba Conference on Multispectral Imaging, Chiba, Japan, 1999.